Article

pubs.acs.org/Biomac

Probing the Impact of Acidification on Spider Silk Assembly Kinetics

Dian Xu,[†] Chengchen Guo,[†] and Gregory P. Holland*[,‡]

[†]Department of Chemistry and Biochemistry, Magnetic Resonance Research Center, Arizona State University, Tempe, Arizona 85287-1604, United States

[‡]Department of Chemistry and Biochemistry, San Diego State University, 5500 Campanile Drive, San Diego, California 92182-1030, United States

Supporting Information

ABSTRACT: Spiders utilize fine adjustment of the physicochemical conditions within its silk spinning system to regulate spidroin assembly into solid silk fibers with outstanding mechanical properties. However, the exact mechanism about which this occurs remains elusive and is still hotly debated. In this study, the effect of acidification on spider silk assembly was investigated on native spidroins from the major ampullate (MA) gland fluid excised from *Latrodectus hesperus* (Black Widow) spiders. Incubating the protein-rich MA silk gland fluid at acidic pH conditions results in the formation of silk fibers that are 10−100 μm in length and ∼2 μm in diameter as judged by optical and electron microscope methods. The in vitro spider silk assembly kinetics were monitored as a function of pH with a ^{13}C solid-state MAS NMR approach. The results confirm the importance of acidic pH in the spider silk self-assembly process with observation of a sigmoidal nucleation-elongation kinetic profile. The rates of nucleation and elongation as well as the percentage of β-sheet structure in the grown fibers depend on the pH. These results confirm the importance of an acidic pH gradient along the spinning duct for spider silk formation and provide a powerful spectroscopic approach to probe the kinetics of spider silk formation under various biochemical conditions.

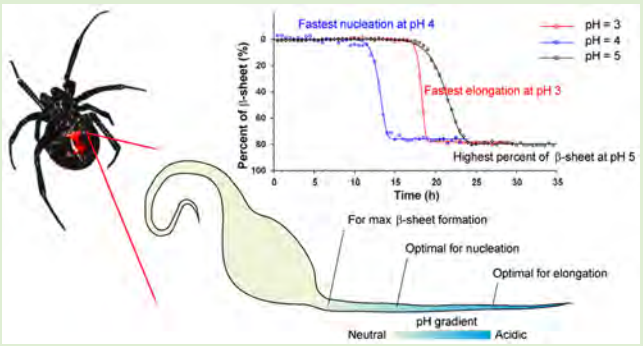

INTRODUCTION

Spiders use up to seven types of silk with a diverse range of physical and mechanical properties to help them survive their environments.[1−3] Each type of silk is a proteinaceous material produced by a specific type of gland inside the spider's abdomen. The dragline spider silk is an outstanding fiber with an extraordinary toughness exceeding man-made fibers such as Kevlar.[1−5] Collectively, spider silk has drawn considerable attention in the field of material science.[6−8] The dragline silk (or major ampullate silk) is particularly attractive because of its exceptional mechanical properties and ease of collection compared to other types of spider silk. To achieve the goal of producing synthetic spider silk with comparable mechanical properties to natural silk, great effort has been made to elucidate the secondary structures and higher order organization of the dragline silk spidroins prior to[9−13] and after[14−28] fiber formation as well as the physicochemical conditions that are responsible for the structural transformation from soluble silk protein to insoluble super fiber.[29−34]

The dragline silk contains primarily two proteins, major ampullate spidroin (MaSp) 1 and 2, which are both biomacromolecules with molecular weights exceeding 250 kDa.[14,15,35] The molecular architecture of the dragline silk spidroins includes a highly repetitive amphiphilic core region flanked by a nonrepetitive hydrophilic N- and C-terminal domain with sequences that are highly conserved across different spider species.[36,37] The dragline silk spidroins are stored in the major ampullate (MA) glands at high concentration (∼25 to 50 wt %),[3] and the core regions of the MaSp proteins were shown with NMR spectroscopy to have no discernible secondary structures,[9,10,12] exhibiting rapid backbone dynamics on the subnanosecond time scale.[13] A Raman spectromicroscopy and circular dichroisim (CD) study also indicates a random coil structure for spider MA silk proteins in the gland with a small population of polyproline II (PPII) and α-helicies.[11] In contrast, the terminal domains appear to be well-structured helical bundles and are proposed to facilitate spidroin assembly via dimerization at acidic pH.[38−43] During the silk protein self-assembly process, it is thought that the spidroins experience changes in physicochemical conditions along the elongated duct to drive silk formation in a controlled manner.[44−46] In the final spun spider silk fiber, the spidroins were shown with X-ray diffraction (XRD) and solid-state NMR methods to form nanocrystalline β-sheet structures aligned along the fiber axis interleaved with more disordered regions that form approximate 3_1-helical and type II β-turn conformations.[16−28]

Received: April 13, 2015
Revised: May 29, 2015

DOI: 10.1021/acs.biomac.5b00487
Biomacromolecules XXXX, XXX, XXX−XXX

Despite the fast progress on characterizing the structures of spidroins in the silk fibers, it is still critical to understand the structural transitions as well as how the self-assembly of spidroins is regulated by changes in physicochemical conditions during the spinning process. In order to elucidate the important physicochemical condition responsible for spider silk spidroin assembly, studies have been done on different systems including spidroin mimics, recombinant spidroins, spidroins regenerated from spider silk or native spidroins from silk glands.[29−34] For example, it has been indicated that the high concentration of sodium chloride in the silk gland helps increase the solubility of the spidroins and prevents undesired aggregation[30,31,34] while, potassium and phosphate ions induce the formation of β-sheet structures.[29,30,34] Additionally, a pH gradient from neutral to acidic conditions was observed from the silk gland to the spinning duct indicating acidification is a critical parameter that drives the assembly of soluble spidroins into silk fibers.[31,34,46] Further, structural information on the recombinant N-terminal domains for spidroins provides an explanation for the mechanism of acidification-assisted spidroin assembly at the molecular level.[39,41−43] In addition, although relatively less studied, the effects of dehydration[44] and shearing force or elongation flow[47] are believed to also be important variables that promote β-sheet formation as well as molecular alignment of the spidroins during the spinning process.

In this work, the impact of acidification on spidroin assembly is investigated for *Latrodectus hesperus* (Black Widow) native MA silk fluid with an in vitro ^{13}C solid-state MAS NMR approach. The spider silk assembly process was investigated at a number of acidic pH conditions. Compared to other characterization techniques, this solid-state NMR method is able to resolve and detect poly(Ala) present in both the liquid (as random coil) and the solid phase (as insoluble β-sheet structures) during fiber assembly. The resulting time-dependent data represents the first illustration of monitoring pH-dependent spider silk assembly kinetics in vitro at near native conditions with a NMR spectroscopic method. The assembly of spider silk fibers from the native MA gland fluid was observed for a range of pH from 3 to 6 with a long period for nucleation followed by a rapid pH-dependent elongation process.

EXPERIMENTAL SECTION

Sample Preparation. *Latrodectus hesperus*, Black Widow (BW), spiders were chosen because of their abundance in the southwestern United States and the complete primary amino acid sequence of both spider silk proteins MaSp1 and MaSp2 is known for this species.[35] Mature female spiders were forcibly silked at a speed of 2 cm/s for a 30 min time period. During the silking process, each spider was fed ∼20 μL 15% (w/v) aqueous solution of uniformly labeled U−^{13}C-L-alanine or U-[^{13}C, ^{15}N]-L-alanine every other day. After 2 weeks of isotope labeling, Ala, Gly, Gln, and Ser are enriched with ^{13}C.[48] The spiders were then sacrificed and dissected under an optical microscope. The intact MA glands were carefully extracted from the spider's abdomen and rinsed with ultrapure water (neutral pH), the ducts, tails, and outside membranes were then gently removed. The gland fluid from four intact MA glands from two isotope enriched BW spiders were transferred into a Bruker Kel-F 4 mm rotor insert filled with an aqueous solution of 5% (w/v) sodium azide (to prevent bacterial growth), 10 mM sodium formate, and 10 mM piperazine buffer solution (as chemical pH indicator).[49] The silk protein concentration is near the native concentration (∼30 wt %) and is approximated to be ∼23 wt % following addition of the buffer. Hydrochloric acid was added to adjust the pH of the buffer. For microscopy imaging, the silk protein solution at a pH = 3 was extracted from the rotor insert following silk fiber formation, as monitored by solid-state NMR experiments. A 10 times diluted and nondiluted silk protein solution was used for optical microscopy and transmission electron microscopy (TEM), respectively.

Polarized Light Microscopy. A total of 1 μL of the silk protein solution was placed on a glass slide and imaged using an Olympus MVX10 Macroview microscope with a SC100 camera. The light was polarized by Olympus polarizer SZX-PO and analyzed by SZX-AN analyzer. Images were taken and analyzed by the Olympus cellSens v1.9 software.

Negative-Staining Transmission Electron Microscopy. A total of 2 μL of the silk protein solution was deposited on a 200 mesh copper grid with a pure carbon support film. After 20 s of slow drying, 10 μL of 2% (w/v) pH = 7.4 phosphotungstic acid (PTA, Ted Pella Inc., Redding, CA) solution was slowly introduced onto the sample for 60 s. The extra solution was gently removed from the side of the grid and the sample was dried at room temperature for 60 s. TEM images were acquired on a Philips CM200 TEM (Philips Electron Optics, Eindhoven, The Netherlands) at 200 kV.

Scanning Electron Microscopy. The dragline silk sample was taped on the sample holder and coated with Au/Pd in a Denton vacuum sputter coater desk II for 120 s under a pressure of 200 mTorr. The deposition rate was 5 nm/min with a current of 20 mA. The SEM image was taken using a FEI XL30 Environmental SEM-FEG. The SEM was operating at a vacuum pressure less than 9×10^{-5} mbar and a beam current of 10.00 kV.

Solid-State NMR. All solid-state NMR experiments were conducted with a 400 MHz Bruker Avance III spectrometer equipped with a 4 mm double-resonance (^{1}H/^{13}C) MAS probe at 25 °C. One-dimensional (1D) ^{13}C direct-detect (DD) MAS NMR spectra were obtained at a 4 kHz MAS frequency with a 90° ^{13}C pulse and 55 kHz TPPM[50] ^{1}H decoupling during acquisition with a 15° phase shift. A total of 256 scans were collected for each spectrum with a 7 s recycle delay (fully relaxed). In order to monitor silk fiber assembly kinetics, consecutive ^{13}C DD-MAS experiments were collected for a set of BW MA gland fluid samples incubated at a pH = 3, 4, and 5 for 24, 28, and 35 h, respectively. To test the impact of MAS on the fiber formation kinetics, a set of 1D ^{13}C DD-MAS NMR spectra were collected without MAS on a control sample incubated at pH = 4 (see Supporting Information). 1D ^{1}H−^{13}C CP-MAS experiments were collected with 4 kHz MAS, a 1 ms ramped (50%) ^{1}H spin-lock pulse with a radio frequency (rf) field of 56.5 kHz matched to the −1 Hartmann−Hahn spinning sideband on the ^{13}C channel. TPPM[50] ^{1}H decoupling was applied during acquisition with a 15° phase shift. The ^{1}H−^{13}C CP-MAS spectra were acquired right after collecting the ^{13}C DD-MAS experiments for samples incubated at a pH = 3, 4, and 5. Another set of samples was incubated at pH = 6 and 7 for 7 days before the ^{1}H−^{13}C CP-MAS experiments were collected.

Two-dimensional (2D) ^{13}C−^{13}C correlation experiments were acquired at a 10 kHz MAS frequency with the DARR ^{13}C−^{13}C recoupling method.[51,52] 150 ms of CW irradiation was applied on the ^{1}H channel at the n = 1 rotary-resonance condition. The acquisition parameters were a 25 kHz sweep width in both dimensions with 512 points in the direct dimension and 196 points in the indirect dimension, 128 scans were averaged with a 2.5 s recycle delay. The 2D DARR experiments were acquired on a BW MA silk gland fluid sample incubated at a pH = 3 for 24 h and native spider dragline silk collected from the same spiders by forcible silking.

Data Processing and Analysis. In order to monitor spider silk assembly kinetics, 48 1D ^{13}C DD-MAS spectra for pH = 4 sample, 56 1D ^{13}C direct spectra for pH = 3 sample and 70 1D ^{13}C direct spectra for pH = 5 sample were collected successively each 30 min following sample preparation. During data processing, all spectra were zero filled to 16 k data points, and a 100 Hz line broadening was applied, followed by baseline correction. To accurately extract the peak intensity of the random coil peak for Ala C_β, the region from 13 to 29 ppm was deconvoluted into the following four peaks, with chemical shifts extracted from the 2D DARR spectrum, Ala C_β at 16.6 ppm (random coil), Ala C_β at 20.5 ppm (antiparallel β-sheet), Ala C_β at 23.0 ppm (parallel β-sheet) and Gln C_β at 26.8 ppm (representative deconvolution of Ala C_β resonance is shown in Figure S1). Spectrum

DOI: 10.1021/acs.biomac.5b00487
Biomacromolecules XXXX, XXX, XXX−XXX

process and deconvolution were accomplished by using the MestReNova v. 8.0.2 data process package.

The kinetic curves were then plotted with the measured peak intensities for the Ala C_β random coil peak as a function of time (see Figures S1 and S2 for justification of using random coil peak intensities). To quantify the kinetic behavior of spider silk fiber formation and better analyze the impact of different pH conditions, a modified Kolmogorov-Johnson-Mehl-Avrami (KJMA) kinetic model[53] from the overall crystallization theory was applied to the experimental data. The general form of the analytical expression for the model is

$$\alpha(t) = 1 - \exp\left[-\left(\frac{t}{\theta}\right)^n\right]$$

where α represents the normalized experimentally observed intensity for Ala C_β random coil peak, θ is a time constant quantifying the time scale of fiber formation, and n is a kinetic index indicating the rate of elongation. To accommodate the model to our experimental data, a slight modification as follows was made to enable applicability of fitting a decreasing sigmoidal curve with nonzero fraction at equilibrium:

$$\alpha(t) = A + (1 - A)\exp\left[-\left(\frac{t}{\theta}\right)^n\right]$$

where an extra parameter, A, was added to better determine the percentage of Ala that did not adopt a β-sheet conformation at equilibrium and remained random coil. The lag time, t_l, and the maximal rate of elongation, k, can be determined based on the following formulas:

$$t_l = \left(\frac{n-1}{n}\right)^{1/n}\left[1 - \frac{e^{n-1/n} - 1}{n-1}\right]\theta$$

$$k = (n-1)\left(\frac{n}{n-1}\right)^{1/n} e^{-n-1/n}\frac{1}{\theta}$$

RESULTS

During the spider silk spinning process, acidic conditions are observed in the duct region with reported pH values from 6.3 to a range of 5 to 4 (or even lower near the spinneret).[43,46,54,55] To examine whether the spidroins within the MA glands can be transformed from an unstructured, random coil state into an assembled fibrous state in vitro via acidification, ^{13}C-L-alanine labeled BW spider MA gland fluid was incubated at 25 °C for 24 h at a pH = 3. Following acidification, a ^{13}C CP-MAS spectrum was collected that exhibits strong CP signals for Ala C_α, C_β, CO and Gly C_α, CO resonances, illustrating that Ala and Gly in the spidroins must adopt a rigid aggregate after being acidified for 24 h (see Figure 1A). The resulting chemical shifts for the Ala and Gly peaks (Table 1) match with the corresponding β-sheet secondary structures. This is consistent with the poly(Ala) and poly(Gly-Ala) regions of the MaSp1 and MaSp2 motifs forming β-sheet structures as is known in native spider silk fibers.[1−3,16,56−71]

2D ^{13}C−^{13}C DARR experiments were conducted to compare the structures between the aggregated spidroins from the acidified gland fluid with the spidroins in the native MA fibers collected from the same spiders (see Figure 1B). The 2D ^{13}C−^{13}C spectra and extracted conformation dependent chemical shifts are strikingly comparable illustrating that the structures formed in the acidified gland fluid are similar to the structures formed in native spider silk fibers. In Figure 1B, the cross peaks for Ala and Gly from aggregated silk gland fluid and silk fibers are overlapped and shown for comparison purposes and compare well. The only difference in the spectra of the native spider silk and the acidified gland fluid is the lower

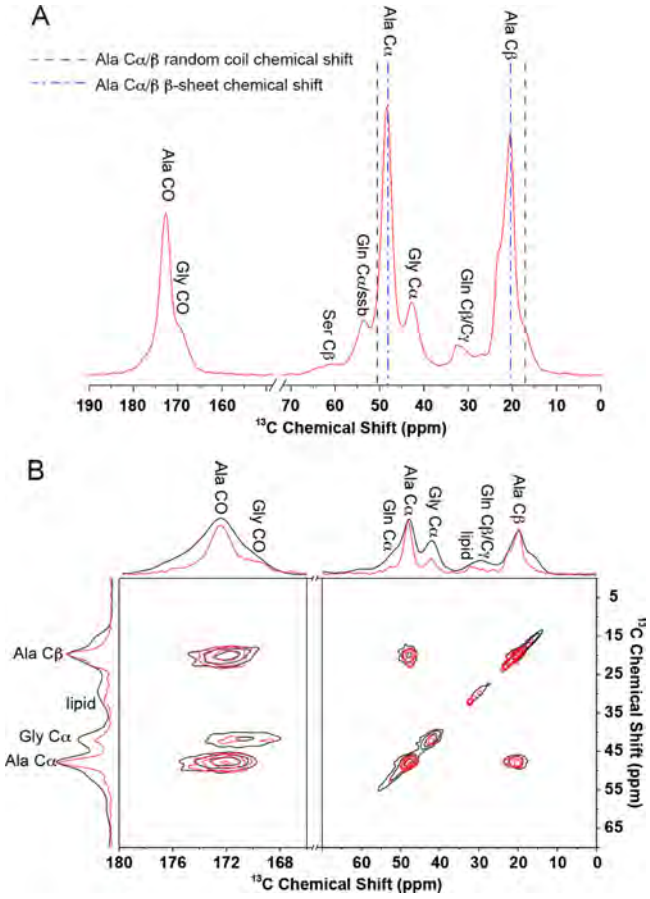

Figure 1. 1D ^{1}H−^{13}C CP MAS spectrum (A) and 2D ^{13}C−^{13}C DARR spectra (B, red) of U−^{13}C-L-alanine labeled BW MA gland fluid incubated at pH = 3 for 24 h. Spectra were collected at 6 kHz for CP-MAS and 10 kHz for DARR experiments. The 2D ^{13}C−^{13}C DARR spectrum of the U−^{13}C-L-alanine labeled BW dragline silk (B, black) was also collected and shown for comparison purposes.

intensity observed for resonances from disordered helical and turn-like domains due to presence of water. Water penetrates these disordered domains increasing local molecular dynamics for these regions with a corresponding decrease in CP efficiency. This is similar to observations made in super-contracted spider dragline silk where the silk is wetted with water.[22,27,72,73]

Optical microscopy and TEM experiments conducted on the acidified gland fluid extracted from the NMR sample at pH = 3 clearly confirm the formation of needle-like fibers 10−100 μm in length (see Figure 2A,B) illustrating that acidification of the gland fluid results in the formation of spider silk fibers. Interestingly, the fiber diameters were measured to be 1.5 ± 0.7 μm using TEM (see Figure 2C) which is very close to the 2.2 ± 0.1 μm diameter of native BW dragline silk fibers (Figure 2D). The large aspect ratio of the fibers formed from the silk gland fluid in the present study suggests that the β-sheet structures are likely to be aligned parallel to the fiber axis as in native spider silk. Although X-ray diffraction data on the fibers is required to confirm the alignment of β-sheet nanostructures, the length of the fibers have made such studies challenging compared to native spider silks.

Different pH conditions ranging from 3 to 7 were investigated to study the impact of pH on spider silk assembly. Separate ^{13}C-L-alanine labeled BW MA silk gland fluid samples

DOI: 10.1021/acs.biomac.5b00487
Biomacromolecules XXXX, XXX, XXX−XXX

Table 1. ^{13}C Chemical Shift of Native Black Widow MA Gland Protein before and after Fiber Formation (Aggregated) At Acidic pH, the Chemical Shifts for Model Peptides with Known Secondary Structures Are Shown for Comparison Purposes[56−71]

	^{13}C chemical shift[a]					
	gland	aggregated	native silk	α-helical	β-sheet	random coil
Ala C_α	50.3	48.3, 49.7	48.6, 49.4, 52.4	52.3−52.8	48.2−49.3	50.5
Ala C_β	16.5	20.5, 16.6	20.4, 17.0, 16.4	14.6−16.0	19.9−20.7	17.1
Ala CO	175.5	172.2	172.4, 175.4	176.2−176.8	172.0−175.2	175.8
Gly C_α	42.9	42.3	41.3, 43.0		43.2−44.3	43.1
Gly CO	171.8	168.9, 171.9	168.8, 171.8		168.4−169.7	172.9
Gln C_α	53.4	53.3	52.4	56.4−57.0	51.0−51.4	54.2
Gln C_β	26.8	26.9	27.4	25.6−26.3	29.0−29.9	27.4
Gln C_γ	31.3	31.2	30.9	29.7−29.8	29.7−29.9	31.7
Gln C_δ	177.8	177.7	177.5			178.5
Gln CO	174.0		172.8	175.4−175.9	171.9−172.2	174.0

[a]All chemical shifts are referenced to TMS.

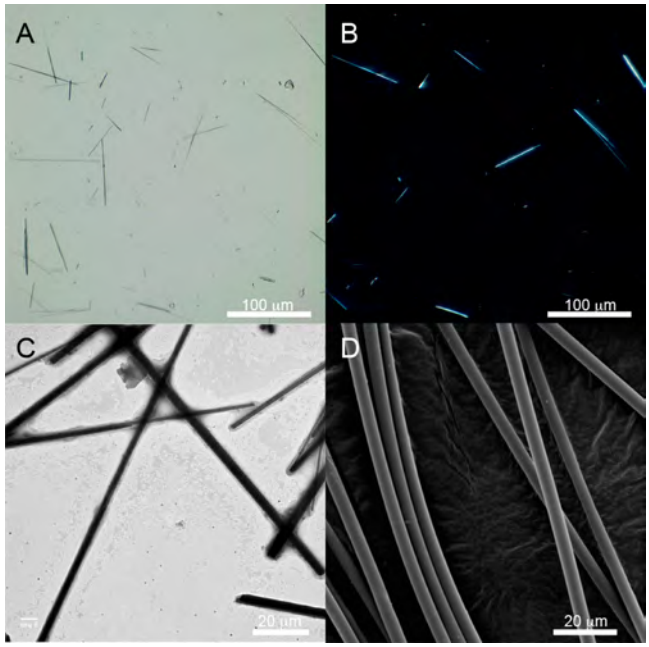

Figure 2. Polarized light microscopy images with (A) and without (B) cross-polars and TEM (C) image for silk fibers formed by incubating the BW MA silk gland fluid at pH = 3 for 24 h. SEM image of BW dragline silk fibers collected from the same spiders (D).

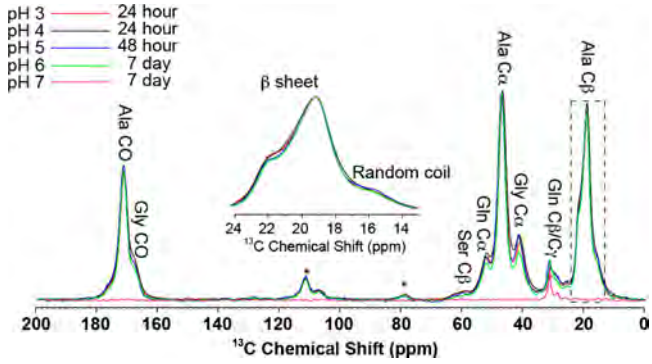

Figure 3. $^{1}H-^{13}C$ CP MAS spectra of U−^{13}C-L-alanine labeled BW MA silk gland fluid following incubation at pH = 3 (red), 4 (black), 5 (blue), 6 (green), and 7 (magenta). Spectra were collected following a 24 h incubation period for pH = 3 and 4, 48 h for pH = 5, and 7 days for pH = 6 and 7 from initial sample preparation.

were prepared and incubated at different pH conditions and 25 °C. In Figure 3, the $^{1}H-^{13}C$ CP-MAS spectra at different pH conditions are shown. At pH = 7, the spidroins remained unstructured for more than 7 days, as no CP signal was detected from the silk proteins. At pHs below 7, the spidroins are assembled into an aggregated fiber with a β-sheet rich conformation. The overlay of the CP spectra at pH below 7 shows no obvious difference in secondary structures. However, at pH = 6, the pH reported for the duct region of the spider silk gland[45,46,55] and the dimerization of the N-terminal domain,[39,41−43] an extremely long period of 7 days is required for the spidroins to self-assemble into the aggregated, fibrous state. In contrast, at more acid environments, the time it takes for the spidroins to aggregate can be greatly reduced to less than 24 h.

The effect of pH on the spider silk spidroin assembly kinetics was monitored with fully relaxed ^{13}C DD-MAS solid-state NMR. For the unstructured spidroins, the ^{13}C DD-MAS spectrum exhibits relatively sharp peaks because of the fast subnanosecond silk protein backbone dynamics in the random coil state (see Figure 4A).[13] However, after the silk fiber is formed, broader peaks are observed with ^{13}C chemical shifts that correspond to β-sheet structures (see Figure 4A). A time period of 24−35 h was required to record the full process of spidroin assembly at different acidic pH conditions from 3 to 6. Consecutive ^{13}C DD-MAS spectra were collected, with each one requiring 30 min to obtain quantifiable ^{13}C spectra with acceptable S/N ratio. The spider silk assembly transition is clearly monitored in the Ala C_β region of the spectrum where a simultaneous increase for the broad β-sheet resonance occurs with a corresponding decrease of the narrow random coil resonance (Figure 4B). The composition of the spidroins with different conformations at each sampling point was further extracted by deconvoluting the Ala C_β region into three peaks (see Figure S1).

The time dependence of the increase of β-sheet components and the decrease of random coil components in the spidroins at pH = 4 is plotted in Figure 5. The trends of the two components are very close, which is further confirmed by applying the kinetic model to the data. The rate constant k for the random coil peak decrease is 0.52 compared to 0.54 for the increase of the β-sheet peak, while the lag times are 12.4 and 12.1 h, respectively (see Table S1). This result indicates the decrease of the random coil component is mainly due to the formation of β-sheet aggregates. Although the increase of the

DOI: 10.1021/acs.biomac.5b00487
Biomacromolecules XXXX, XXX, XXX−XXX

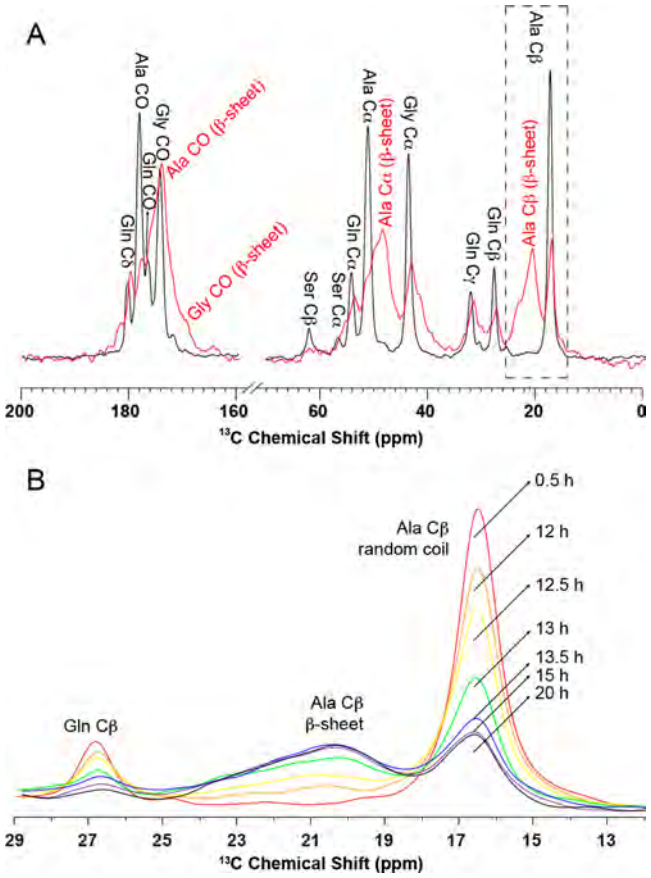

Figure 4. ^{13}C DD-MAS NMR spectra of U−^{13}C-L-alanine labeled BW MA silk gland fluid at pH = 4 before (A, black) and after spider silk assembly (A, red). The Ala C_β region is framed by dashed lines and will be analyzed to monitor spider silk assembly kinetics. Ala C_β regions from the ^{13}C DD-MAS spectra collected at different time from sample preparation were stacked showing that the decrease for the random coil resonance and increase for the β-sheet resonance can be observed simultaneously as a function of time (B).

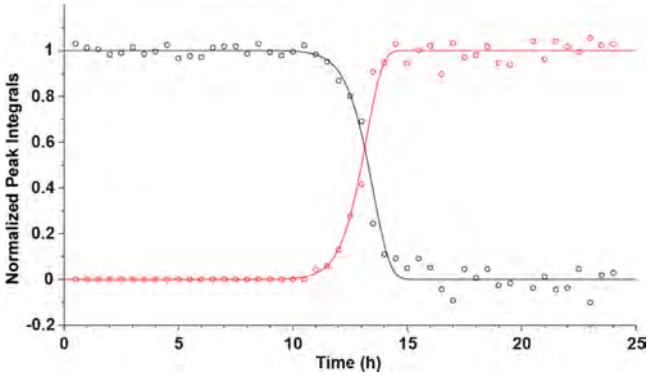

Figure 5. Time dependence of normalized peak integrals for random coil peak (black circle) and β-sheet peak (red circle) from the kinetic measurement of spider silk fiber formation for U−^{13}C-L-alanine labeled BW MA gland fluid at pH = 4 with ^{13}C DD-MAS NMR. The data was fit to modified KJMA kinetic model and the extracted kinetic parameters are shown in Table S1.

broad peak for β-sheet conformation can be observed by solid-state NMR spectroscopy, it is advantageous to indirectly track the spidroin assembly by monitoring the decrease of the much narrower and intense random coil resonance to gain better sensitivity. In addition, it is worth noting that the agreement between the random coil decay and β-sheet build-up kinetics indicates that the vast majority of the NMR signal is observed in the ^{13}C DD-MAS spectrum of native BW MA silk proteins prior to fiber formation and corroborates previous interpretations.[13]

The kinetic curves for spider silk assembly at different pH were established by plotting the normalized peak intensities of the random coil peak for the Ala C_β as a function of time. A signature sigmoidal shaped kinetic curve was observed for the spider silk assembly process for the three acidic pHs tested (see Figure 6). A long lag time was observed followed by rapid

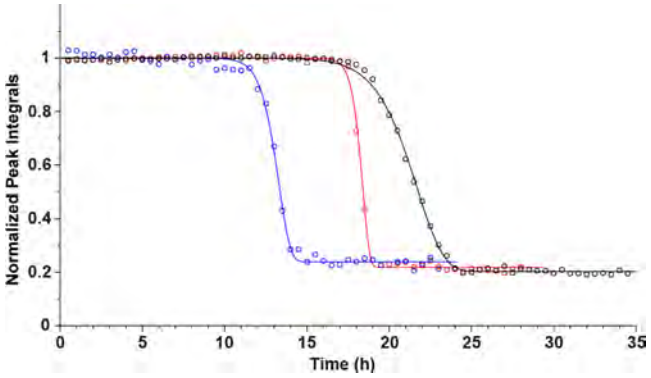

Figure 6. Kinetic curves for U−^{13}C-L-alanine labeled BW MA silk gland fluid incubated at pH = 3 (red circle), 4 (blue circle) and 5 (black circle). The solid curves were obtained by applying the modified KJMA model and the extracted kinetic parameters are shown in Table 2.

elongation indicating that nucleation is a prerequisite. The impact of pH on the different phases of spidroin fiber formation can be analyzed by applying the modified KJMA model to the kinetic curves (Table 2). At pH = 4, the shortest lag time (12.1 h) is required for the spidroins to shift to the rapid elongation phase. However, an extra 5.5 or 7 h was observed for passing the nucleation phase at pH = 3 or 5. Although the nucleation phase took a longer time at pH = 5, the β-sheet conformation yielded the largest percentage (80%) of Ala in a β-sheet structure at equilibrium suggesting longer nucleation times is beneficial for the complete formation of crystalline β-sheet components. However, the difference in the fraction of Ala that forms a β-sheet structure at different acidic pHs is small ranging from 70 to 80% and not far off from the fraction of Ala in β-sheet structures from solid-state NMR studies on native BW MA silk fibers where it was determined to be 88%.[28] The increasing rate constants of the elongation phase from 0.24 to 0.91 with decreasing pH values from 5 to 3 indicates that the elongation process is accelerated by more acidic conditions.

DISCUSSION

The ^{13}C DD-MAS NMR spectrum of the BW spidroins within the MA glands displays narrow resonances, with chemical shifts matching a random coil structure. Although the spidroins are stored in the silk glands at a near neutral but slightly acidic environment (pH ~ 6.3), a high concentration of NaCl (~180 mM) is present and believed to prevent premature aggregation and maintain an unstructured, random coil state.[45] It has been proposed that an acidic pH gradient exists in the spinning system from the silk glands along the duct to the spinneret and is likely important for spider silk formation.[46,54] With the

DOI: 10.1021/acs.biomac.5b00487
Biomacromolecules XXXX, XXX, XXX−XXX

Table 2. Fitting Parameters from the Kinetic Curves Using a Modified KJMA Model for Spider Silk Fiber Assembly at Different pH Conditions and Different MAS Frequencies

pH	n	θ	A	k	t_1
3 (4 kHz MAS)	45.5 ± 3.6	18.4 ± 0.1	0.22 ± 0.01	0.91 ± 0.07	17.7 ± 0.1
4 (4 kHz MAS)	19.8 ± 2.5	13.3 ± 0.1	0.24 ± 0.01	0.55 ± 0.07	12.1 ± 0.2
5 (4 kHz MAS)	14.2 ± 0.5	21.8 ± 0.1	0.20 ± 0.01	0.24 ± 0.01	19.2 ± 0.1
4 (0 kHz MAS)	19.7 ± 2.8	13.2 ± 0.1	0.30 ± 0.01	0.55 ± 0.08	12.1 ± 0.2

limitation of experimental methods, accurate measurement to map out the pH values in the spinning system is still challenging. However, the spidroins are expected to experience much lower pH values near the spinneret.[55] In addition, to induce fiber formation in vitro on the native spider silk gland fluid with a high NaCl content, a lower pH condition may be required compared to the in vivo spinning conditions. Therefore, to study the effect of acidic biochemical conditions on spider silk fiber formation, acidic conditions from pH = 6 to 3 were investigated for the native BW MA spidroins. At pH = 7, the spidroins remain unstructured random coils for over 7 days with no evidence of aggregation, but when acidic conditions are applied, the metastable state of the unstructured spidroins is disturbed and aggregation to silk fibers occurs albeit with different kinetics. The spidroins assemble into fibers at pH $\leq$ 6, with no observable difference in the conformational structures of the folded spidroins for different pH values following fiber formation. However, distinguishable difference in the rates of fiber formation from 7 days at pH = 6 to 12 h at pH = 4 are observed leading to the study on the kinetics of spidroin fiber formation at acidic conditions with ^{13}C DD-MAS NMR.

The kinetic profile of spidroin fiber formation is a typical sigmoidal curve. The long period of lag time indicates nucleation is required to allow further elongation. Unlike a parabolic curve, the sigmoidal curve also indicates no seeds existed in the system to help skip the nucleation phase.[74] Because nucleation is a crucial prerequisite for fiber formation, it was important to determine that centrifugal and centripetal forces from MAS did not influence the kinetics to any appreciable extent as confirmed by the static ^{13}C NMR experiments (see Figure S3 and Table 2). Comparison of the extracted kinetic parameter for static and 4 kHz MAS conditions illustrates that MAS has little impact on the spider silk assembly kinetics with the exception of a slightly higher remaining random coil fraction of 0.30 and 0.24 at equilibrium for the two conditions, respectively.

The lag times observed for spider silk fiber formation as a function of pH in the present study are surprisingly long (>12 h) indicating that pH may not be the biochemical variable that controls nucleation. Previous studies on silkworm fibroins and spider spidroins indicate shorter lag times for fiber formation.[29,30,34,75] These previous studies are likely not comparable to the investigation here because of the dilute (~0.1% by wt) protein concentrations used compared to the much higher concentration of silk proteins (~23% by wt) in the silk glands used in this study. Even though the remaining NaCl in the silk gland may postpone nucleation, the over 12 h of lag time implies that other mechanisms may be responsible for nucleation. One possible explanation for this is the gel-like state of spider silk spidroins inside the MA gland that can prevent or postpone nucleation. Thus, any approaches to dissolve the dope inside silk glands will remove this stabilizing effect of the gel-like state with high salt content leading to faster aggregation due to increased hydrophobic interactions. Similarly, one must consider the other physicochemical influences such as dehydration, shearing forces and the influence of other ions that could be introduced in the duct to assist the nucleation process.[29−31,34,44,46,47]

As shown in Figure 6, the shortest nucleation phase was observed at a pH near the isoelectric point (pI = 4.25) of the N-terminal domains (NTD) of the spidroins.[38] This result indicates the nucleation process may be related to the NTD. The NTD is known to dimerize at a pH = 6 and the dimerization becomes more stable as pH decreases.[39,41,43] Compared to a pH = 3 or 5, the solubility of the NTD dimer is much lower at a pH = 4. This is consistent with the results presented here where the shortest nucleation phase is observed at a pH = 4. In comparison, during the elongation process, the spidroins exhibit the fastest elongation rate at lower pH values. Since the pI of the entire silk protein was experimentally estimated to be ~4.2,[30,31] the fastest rate of elongation phase at pH = 3 implies that the elongation phase is not governed by the solubility change of the entire silk protein. In addition, a larger percent of β-sheet structures is formed in the silk fibers with longer nucleation time. Combining the information listed above, it is reasonable to propose a possible model to explain the function of the pH gradient in the spinning system. The spidroins are initially stored in an unstructured, random coil state at near neutral pH, where the spidroins can remain stable. At pH = 6, the NTD first starts to form dimers followed by silk protein nucleation. Larger assemblies are formed at a pH ~ 5 to ensure higher percentage of β-sheet structures in the silk fiber, then the solubility of the silk protein drops dramatically at a pH = 4 leading to rapid fiber formation. When the dope is close to the spinneret, decreasing the pH below 4 can accelerate the elongation rate even further. Thus, a pH gradient can be used to regulate the speed of the nucleation and elongation as well as the final β-sheet composition in the spider silk assembly process. Lastly, although pH appears to be important in regulating and controlling spider silk assembly, the other physicochemical variables that have been discussed previously[29−31,34,44,46,47] will certainly contribute to the assembly process.

CONCLUSIONS

The kinetics of spider silk assembly were tracked with solid-state NMR spectroscopy for native BW MA silk proteins as a function of pH. The resulting kinetic profiles reveal that silk fiber formation is nucleation dependent and the rate of nucleation reaches a maximum when the pH value is close to the pI of the N-terminal domain and the silk protein. In addition, decreasing the pH value can accelerate the rate of elongation while, a higher percentage of the spidroins was observed to exhibit a β-sheet conformation in the silk fiber at less acidic conditions. Therefore, the gradual pH decrease along the duct can be used to optimize the speed of silk production as well as to achieve higher crystalline compositions in the final fibers. We anticipate that this in vitro ^{13}C solid-state NMR

DOI: 10.1021/acs.biomac.5b00487
Biomacromolecules XXXX, XXX, XXX−XXX

approach will be a valuable tool moving forward to interrogate a range of biochemical conditions on spider silk assembly including the effect of various salts. Such studies are already under way in our laboratory.

■ ASSOCIATED CONTENT

Supporting Information

KJMA kinetic parameters for Ala C_β random coil and β-sheet component from ^{13}C DD-MAS NMR kinetic curves obtained during acidification; an example of peak deconvolution for the Ala C_β region from the ^{13}C DD-MAS NMR spectrum; kinetic curves for the spider silk protein assembly with and without MAS. The Supporting Information is available free of charge on the ACS Publications website at DOI: 10.1021/acs.biomac.5b00487.

■ AUTHOR INFORMATION

Corresponding Author

*E-mail: gholland@mail.sdsu.edu.

Notes

The authors declare no competing financial interest.

■ ACKNOWLEDGMENTS

This work was supported by grants from the Department of Defense Air Force Office of Scientific Research (AFOSR) under Award No. FA9550-14-1-0014, the Defense University Research Instrumentation Program (DURIP) under Award No. FA2386-12-1-3031 DURIP 12RSL231, and the National Science Foundation, Division of Materials Research (NSF-DMR) under Award No. DMR-1264801. We thank Dr. Brian Cherry for help with NMR instrumentation and student training.

■ ABBREVIATIONS

CP, cross-polarization; MAS, magic angle spinning; TPPM, two pulse phase modulation; DARR, dipolar assisted rotational resonance; CW, continuous wave

■ REFERENCES

(1) Gosline, J. M.; Demont, M. E.; Denny, M. W. *Endeavour* **1986**, *10*, 37−43.
(2) Altman, G. H.; Diaz, F.; Jakuba, C.; Calabro, T.; Horan, R. L.; Chen, J. S.; Lu, H.; Richmond, J.; Kaplan, D. L. *Biomaterials* **2003**, *24*, 401−416.
(3) Lewis, R. V. *Chem. Rev.* **2006**, *106*, 3762−3774.
(4) Gosline, J. M.; Denny, M. W.; Demont, M. E. *Nature* **1984**, *309*, 551−552.
(5) Vollrath, F.; Porter, D. *Soft Matter* **2006**, *2*, 377−385.
(6) Teule, F.; Cooper, A. R.; Furin, W. A.; Bittencourt, D.; Rech, E. L.; Brooks, A.; Lewis, R. V. *Nat. Protoc.* **2009**, *4*, 341−355.
(7) Vollrath, F.; Porter, D. *Polymer* **2009**, *50*, 5623−5632.
(8) Omenetto, F. G.; Kaplan, D. L. *Science* **2010**, *329*, 528−531.
(9) Hijirida, D. H.; Do, K. G.; Michal, C.; Wong, S.; Zax, D.; Jelinski, L. W. *Biophys. J.* **1996**, *71*, 3442−3447.
(10) Hronska, M.; van Beek, J. D.; Williamson, P. T. F.; Vollrath, F.; Meier, B. H. *Biomacromolecules* **2004**, *5*, 834−839.
(11) Lefevre, T.; Leclerc, J.; Rioux-Dube, J. F.; Buffeteau, T.; Paquin, M. C.; Rousseau, M. E.; Cloutier, I.; Auger, M.; Gagne, S. M.; Boudreault, S.; Cloutier, C.; Pezolet, M. *Biomacromolecules* **2007**, *8*, 2342−2344.
(12) Jenkins, J. E.; Holland, G. P.; Yarger, J. L. *Soft Matter* **2012**, *8*, 1947−1954.
(13) Xu, D.; Yarger, J. L.; Holland, G. P. *Polymer* **2014**, *55*, 3879−3885.
(14) Xu, M.; Lewis, R. V. *Proc. Natl. Acad. Sci. U.S.A.* **1990**, *87*, 7120−7124.
(15) Hinman, M. B.; Lewis, R. V. *J. Biol. Chem.* **1992**, *267*, 19320−19324.
(16) Simmons, A.; Ray, E.; Jelinski, L. W. *Macromolecules* **1994**, *27*, 5235−5237.
(17) Kummerlen, J.; van Beek, J. D.; Vollrath, F.; Meier, B. H. *Macromolecules* **1996**, *29*, 2920−2928.
(18) Bram, A.; Branden, C. I.; Craig, C.; Snigireva, I.; Riekel, C. *J. Appl. Crystallogr.* **1997**, *30*, 390−392.
(19) Grubb, D. T.; Jelinski, L. W. *Macromolecules* **1997**, *30*, 2860−2867.
(20) Riekel, C.; Vollrath, F. *Int. J. Biol. Macromol.* **2001**, *29*, 203−210.
(21) van Beek, J. D.; Hess, S.; Vollrath, F.; Meier, B. H. *Proc. Natl. Acad. Sci. U.S.A.* **2002**, *99*, 10266−10271.
(22) Holland, G. P.; Lewis, R. V.; Yarger, J. L. *J. Am. Chem. Soc.* **2004**, *126*, 5867−5872.
(23) Holland, G. P.; Creager, M. S.; Jenkins, J. E.; Lewis, R. V.; Yarger, J. L. *J. Am. Chem. Soc.* **2008**, *130*, 9871−9877.
(24) Holland, G. P.; Jenkins, J. E.; Creager, M. S.; Lewis, R. V.; Yarger, J. L. *Chem. Commun.* **2008**, 5568−5570.
(25) Holland, G. P.; Jenkins, J. E.; Creager, M. S.; Lewis, R. V.; Yarger, J. L. *Biomacromolecules* **2008**, *9*, 651−657.
(26) Jenkins, J. E.; Creager, M. S.; Butler, E. B.; Lewis, R. V.; Yarger, J. L.; Holland, G. P. *Chem. Commun.* **2010**, *46*, 6714−6716.
(27) Jenkins, J. E.; Creager, M. S.; Lewis, R. V.; Holland, G. P.; Yarger, J. L. *Biomacromolecules* **2010**, *11*, 192−200.
(28) Jenkins, J. E.; Sampath, S.; Butler, E.; Kim, J.; Henning, R. W.; Holland, G. P.; Yarger, J. L. *Biomacromolecules* **2013**, *14*, 3472−3483.
(29) Chen, X.; Knight, D. P.; Shao, Z. Z.; Vollrath, F. *Biochemistry* **2002**, *41*, 14944−14950.
(30) Dicko, C.; Kenney, J. M.; Knight, D.; Vollrath, F. *Biochemistry* **2004**, *43*, 14080−14087.
(31) Foo, C. W. P.; Bini, E.; Hensman, J.; Knight, D. P.; Lewis, R. V.; Kaplan, D. L. *Appl. Phys. A: Mater. Sci. Process.* **2006**, *82*, 223−233.
(32) Lefevre, T.; Boudreault, S.; Cloutier, C.; Pezolet, M. *Biomacromolecules* **2008**, *9*, 2399−2407.
(33) Lefevre, T.; Boudreault, S.; Cloutier, C.; Pezolet, M. *J. Mol. Biol.* **2011**, *405*, 238−253.
(34) Leclerc, J.; Lefevre, T.; Gauthier, M.; Gagne, S. M.; Auger, M. *Biopolymers* **2013**, *99*, 582−593.
(35) Ayoub, N. A.; Garb, J. E.; Tinghitella, R. M.; Collin, M. A.; Hayashi, C. Y. *PloS One* **2007**, *2*, e514.
(36) Beckwitt, R.; Arcidiacono, S. *J. Biol. Chem.* **1994**, *269*, 6661−6663.
(37) Motriuk-Smith, D.; Smith, A.; Hayashi, C. Y.; Lewis, R. V. *Biomacromolecules* **2005**, *6*, 3152−3159.
(38) Askarieh, G.; Hedhammar, M.; Nordling, K.; Saenz, A.; Casals, C.; Rising, A.; Johansson, J.; Knight, S. D. *Nature* **2010**, *465*, 236−U125.
(39) Gaines, W. A.; Sehorn, M. G.; Marcotte, W. R. *J. Biol. Chem.* **2010**, *285*, 40745−40753.
(40) Hagn, F.; Eisoldt, L.; Hardy, J. G.; Vendrely, C.; Coles, M.; Scheibel, T.; Kessler, H. *Nature* **2010**, *465*, 239−U131.
(41) Hagn, F.; Thamm, C.; Scheibel, T.; Kessler, H. *Angew. Chem.* **2011**, *50*, 310−313.
(42) Schwarze, S.; Zwettler, F. U.; Johnson, C. M.; Neuweiler, H. *Nat. Commun.* **2013**, *4*, 2815.
(43) Kronqvist, N.; Otikovs, M.; Chmyrov, V.; Chen, G.; Andersson, M.; Nordling, K.; Landreh, M.; Sarr, M.; Jornvall, H.; Wennmalm, S.; Widengren, J.; Meng, Q.; Rising, A.; Otzen, D.; Knight, S. D.; Jaudzems, K.; Johansson, J. *Nat. Commun.* **2014**, *5*, 3254.
(44) Tillinghast, E. K.; Chase, S. F.; Townley, M. A. *J. Insect. Physiol.* **1984**, *30*, 591−596.
(45) Knight, D. P.; Vollrath, F. *Naturwissenschaften* **2001**, *88*, 179−182.
(46) Dicko, C.; Vollrath, F.; Kenney, J. M. *Biomacromolecules* **2004**, *5*, 704−710.

DOI: 10.1021/acs.biomac.5b00487
Biomacromolecules XXXX, XXX, XXX−XXX

(47) Boulet-Audet, M.; Terry, A. E.; Vollrath, F.; Holland, C. *Acta Biomater.* **2014**, *10*, 776−784.
(48) Shi, X. Y.; Yarger, J. L.; Holland, G. P. *Anal. Bioanal. Chem.* **2013**, *405*, 3997−4008.
(49) Baryshnikova, O. K.; Williams, T. C.; Sykes, B. D. *J. Biomol. NMR* **2008**, *41*, 5−7.
(50) Bennett, A. E.; Rienstra, C. M.; Auger, M.; Lakshmi, K. V.; Griffin, R. G. *J. Chem. Phys.* **1995**, *103*, 6951−6958.
(51) Takegoshi, K.; Nakamura, S.; Terao, T. *Chem. Phys. Lett.* **2001**, *344*, 631−637.
(52) Takegoshi, K.; Nakamura, S.; Terao, T. *J. Chem. Phys.* **2003**, *118*, 2325−2341.
(53) Auer, S.; Kashchiev, D. *Proteins* **2010**, *78*, 2412−2416.
(54) Vollrath, F.; Knight, D. P.; Hu, X. W. *Proc. R. Soc. B* **1998**, *265*, 817−820.
(55) Andersson, M.; Chen, G.; Otikovs, M.; Landreh, M.; Nordling, K.; Kronqvist, N.; Westermark, P.; Jörnvall, H.; Knight, S.; Ridderstråle, Y.; Holm, L.; Meng, Q.; Jaudzems, K.; Chesler, M.; Johansson, J.; Rising, A. *PLoS Biol.* **2014**, *12*, e1001921.
(56) Kricheldorf, H. R.; Muller, D. *Macromolecules* **1983**, *16*, 615−623.
(57) Saito, H.; Tabeta, R.; Asakura, T.; Iwanaga, Y.; Shoji, A.; Ozaki, T.; Ando, I. *Macromolecules* **1984**, *17*, 1405−1412.
(58) Shoji, A.; Ozaki, T.; Saito, H.; Tabeta, R.; Ando, I. *Macromolecules* **1984**, *17*, 1472−1479.
(59) Saito, H. *Magn. Reson. Chem.* **1986**, *24*, 835−852.
(60) Ishida, M.; Asakura, T.; Yokoi, M.; Saito, H. *Macromolecules* **1990**, *23*, 88−94.
(61) Wishart, D. S.; Bigam, C. G.; Holm, A.; Hodges, R. S.; Sykes, B. D. *J. Biomol. NMR* **1995**, *5*, 67−81.
(62) Asakura, T.; Demura, M.; Date, T.; Miyashita, N.; Ogawa, K.; Williamson, M. P. *Biopolymers* **1997**, *41*, 193−203.
(63) Asakura, T.; Ashida, J.; Yamane, T.; Kameda, T.; Nakazawa, Y.; Ohgo, K.; Komatsu, K. *J. Mol. Biol.* **2001**, *306*, 291−305.
(64) Zhao, C. H.; Asakura, T. *Prog. Nucl. Magn. Reson. Spectrosc.* **2001**, *39*, 301−352.
(65) Asakura, T.; Yao, J. M. *Protein Sci.* **2002**, *11*, 2706−2713.
(66) Murata, K.; Kuroki, S.; Ando, I. *Polymer* **2002**, *43*, 6871−6878.
(67) Ashida, J.; Ohgo, K.; Komatsu, K.; Kubota, A.; Asakura, T. *J. Biomol. NMR* **2003**, *25*, 91−103.
(68) Kishi, S.; Santos, A.; Ishii, O.; Ishikawa, K.; Kunieda, S.; Kimura, H.; Shoji, A. *J. Mol. Struct.* **2003**, *649*, 155−167.
(69) Wildman, K. A. H.; Wilson, E. E.; Lee, D. K.; Ramamoorthy, A. *Solid State Nucl. Magn. Reson.* **2003**, *24*, 94−109.
(70) Asakura, T.; Nakazawa, Y.; Ohnishi, E.; Moro, F. *Protein Sci.* **2005**, *14*, 2654−2657.
(71) Asakura, T.; Yang, M. Y.; Kawase, T.; Nakazawa, Y. *Macromolecules* **2005**, *38*, 3356−3363.
(72) Creager, M. S.; Jenkins, J. E.; Thagard-Yeaman, L. A.; Brooks, A. E.; Jones, J. A.; Lewis, R. V.; Holland, G. P.; Yarger, J. L. *Biomacromolecules* **2010**, *11*, 2039−2043.
(73) Yang, Z. T.; Liivak, O.; Seidel, A.; LaVerde, G.; Zax, D. B.; Jelinski, L. W. *J. Am. Chem. Soc.* **2000**, *122*, 9019−9025.
(74) Morris, A. M.; Watzky, M. A.; Finke, R. G. *Biochim. Biophys. Acta* **2009**, *1794*, 375−397.
(75) Chen, X.; Shao, Z. Z.; Knight, D. P.; Vollrath, F. *Proteins* **2007**, *68*, 223−231.

DOI: 10.1021/acs.biomac.5b00487
Biomacromolecules XXXX, XXX, XXX−XXX